GENERATION AND INJECTION OF E.M. WAVES IN SPACE PLASMA BY MEANS OF A LONG ORBITING TETHER

Contract NAS8-33520

Semiannual Progress Report No. 1

For the period 11 December 1979 to 10 June 1980

July 1980

Prepared for

National Aeronautics and Space Administration

George C. Marshall Space Flight Center

Marshall Space Flight Center, Alabama 35812

Smithsonian Institution
Astrophysical Observatory
Cambridge, Massachusetts 02138

The Smithsonian Astrophysical Observatory and the Harvard College Observatory are members of the Center for Astrophysics

GENERATION AND INJECTION OF E.M. WAVES IN SPACE PLASMA BY MEANS OF A LONG ORBITING TETHER

Contract NAS8-33520

Semiannual Progress Report No. 1

For the period 11 December 1979 to 10 June 1980

July 1980

Prepared for

National Aeronautics and Space Administration

George C. Marshall Space Flight Center

Marshall Space Flight Center, Alabama 35812

Smithsonian Institution
Astrophysical Observatory
Cambridge, Massachusetts 02138

The Smithsonian Astrophysical Observatory
and the Harvard College Observatory
are members of the
Center for Astrophysics

Authorship

The author of this report is Dr. Marino Dobrowolny, Visiting Scientist at Smithsonian Astrophysical Observatory from Laboratorio Plasma Spazio, CNR, Frascati, Italy.

Foreword

This semiannual report fulfills the contractural obligations to date of the Smithsonian Astrophysical Observatory for contract NAS8-33520. Dr. Mario D. Grossi served as Principle Investigator and Mr. Richard S. Taylor as Program Manager. Dr. William S. Johnson, Code ES01, NASA-MSFC, was the Technical Monitor and the Contracting Officer Representative (COR) for this program.

Executive Summary

The long term goals of the theoretical investigation reported herewith on the generation and injection of e.m. waves in space plasma by means of a long orbiting tether, are the following:

a) to provide an estimate of the portions of the primary electrodynamic power developed by the tether, that goes to excite each of various wave generation and injection mechanisms that are expected to be present during a tether's orbital flight;

b) to perform an evaluation of the signal levels associated with each one of the mechanisms above, and to verify their detectability with state-of-the-art instrumentation on the earth surface or elsewhere.

The answers to the questions above will be fundamental inputs to the planning of the observational program to be executed on the occasion of an electrodynamic experiment that will use Shuttle-based T.S.S. facilities.

This semiannual report illustrates the first steps in this path. During the contractual activity, we have identified the generation and injection of Alfvèn waves and electron whistler waves as the most relevant mechanisms activited by the electrodynamic tether. We have also investigated the physical mechanisms that govern these two families of phenomena and we have derived the ratio between the power that goes in Alfvèn waves and in whistlers.

We have also initiated the analysis of the possible production of accelerated electrons by the electrodynamic tether. This analysis will be a main thrust of the project activity in the second half of the contract performance period.

The Final Report will illustrate the physical principles involved in the generation of accelerated electron beams, which in turn, may produce waves through plasma instabilities. Answers to questions a) and b) above will be given with first-cut estimates of the power repartition among the various mechanisms involved. Estimates of the expected signal levels will be included.

The Final Report will also outline a recommended continuation of the effort, aimed at the further development of the first-cut estimates above toward more reliable predictions of the experiment outcome.

Table of Contents

1. Introduction. 1

2. Calculations of current in the tether from charged particle collection. 3

3. Discussion on possible waves radiated by the moving tether. 6

4. Parallel current associated with Alfvèn waves 11

5. Power and impedance associated with Alfvèn waves. 14

6. Comparison of Alfvènic current with current due to charged particle collection. 17

7. Reconsideration of power associated with Alfvèn waves 18

8. Physical picture of the Alfvèn wave system associated with the tether 19

9. Power, current and impedance for parallel electron whistler waves 22

10. Comparison between Alfvèn waves and whistler wave impedance 24

11. Conclusions and comments on future developments 25

12. References. 27

1. Introduction

In previous work on the electrodynamic tether developed at SAO (Dobrowolny et al., 1976; Anderson et al., 1979), we have been mainly concerned in studying current and potential distributions on the tether by using models of charged particle collection from the surrounding ionospheric plasma. This was originally done for the purpose of computing electrodynamic forces on the tether system (Dobrowolny et al., 1976) to be included in a quantitative description of the system dynamics (Kalaghan et al., 1978; Anderson et al., 1979). Both the cases of a bare metallic tether and of a metallic tether covered by an insulator and with conducting electrodes at the ends, were considered in these studies.

On the other hand, these analysis have not touched upon the problem of the perturbations produced by the moving tether in the ionosphere and, consequently, on the more particular issue of where the current of the tether goes in the surrounding medium.

The motion of the conducting tether generates in fact wave perturbations in the medium and the current in the tether is, so to say, continued in the medium through the action of these waves. Some qualitative thoughts about the problem of wave generation have been given in a recent report (Dobrowolny et al., 1979) and, in particular, analogies between possible phenomena produced by the electrodynamic tether and phenomena produced by Jupiter's satellite Io, moving in the Jovian magnetosphere, have been indicated.

The system considered in this report is a metallic tether covered by an insulator, with conducting electrodes (the Shuttle and a conducting balloon) at its terminations. The report is essentially concentrating on the problem of wave generation.

First, we derive new results on the current in the tether-balloon system due to charged particle collection from the ionospheric medium (Sect. 2). These results, which have been obtained with a newly developed method (Arnold and Dobrowolny, 1979), are needed for comparison with the calculations of currents carried away from the tether system through possible waves. A discussion of the range of frequencies of the possible generated waves is then given (Sect. 3).

In Sects. 4 and 5, we derive current, power and impedance associated with transmission of Alfvèn waves from the tether. The Alfvènic current, which flows essentially along the magnetic flux tubes intercepted by the end electrodes and is a function of balloon radius, is then compared (Sect. 6) with the current values obtained from the model of particle collection. The conclusion is that the latter current is always smaller than the Alfvènic current (also for very large balloon dimensions). This leads to a re-estimation of the power transmitted by Alfvèn waves, given in Sect. 7. Section 8 considers the problem of Alfvènic reflection from the ionospheric E layer. Considerations of the transit time of the waves between the region of generation and the E layer, indicate clearly that the reflected waves do not reach the system anymore. Thus, there is no freezing with the tether system of the intercepted flux tubes. The tether, during its motion, generates Alfvèn waves which are then partially reflected between conjugate E layer zones until their amplitude dies down.

The next section (Sect. 9) deals with calculations of power, current and impedance for whistler waves propagating parallel to the magnetic field. A comparison of the whistler waves impedance (a function of frequency ω) with the Alfvèn wave impedance (Sect. 10), shows that the

first is much greater than the second for all whistler frequencies (except those very close to the ion cyclotron frequency). This tells us that, for a given polarization electric field applied, most of the power transmitted in waves by the tether should go into low frequency Alfvèn waves rather than whistler waves. Finally, in Sect. 11, we comment on future developments in the framework of this study.

2. Calculations of current in the tether from charged particle collection.

In this section we will give results for the current in the tether system obtained by considering only the collection of charged particles of the medium from the two conducting electrodes at the ends (the Shuttle and the balloon) and without considering the possibility of wave generation.

The condition that one imposes to derive current and potentials is that of balance of charged particle fluxes between the two end electrodes. In terms of currents, the current collected at the Shuttle i_s has to be equal and opposite to the current i_B collected at the balloon

$$i_s(V_s) = -i_B(V_B) \tag{2.1}$$

(for a tether system without any gun, ion or electron, at the Shuttle). In (2.1) we have explicitly indicated that the currents are functions of the potentials (V_s, V_B) of the two electrodes with respect to the plasma. For a perfectly conducting tether, it would be

$$|V_s - V_B| = |\underline{V}_o \times \underline{B} \cdot L| \tag{2.2}$$

where $\underline{V}_o$ is the Shuttle velocity (V_o = 7.8 km/sec), $\underline{B}$ the earth's magnetic field ($B \sim 0.3$ gauss, at the altitudes of interest between 100 and 300 km) and L is the tether's length. Hence (2.1) is an implicit equation for one

of the potentials, for example V_s. Having determined V_s, V_B is obtained from (2.2) and then the current $I_c = |i_s| = |i_B|$ is calculated from the solutions found for the potentials.

The model which has been used for charged particle collection is the following (Anderson et al., 1979). For the attracted particle contribution to the current referring to particles of species j (j = i, e for ions and electrons respectively), we write

$$\frac{i_j \text{ attracted}}{i_{jo}} = f(V) \tag{2.3}$$

where the normalizing electron and ion currents are given by

$$i_{eo} = \frac{1}{8} n |e| v_{the} A \tag{2.4}$$

$$i_{io} = \frac{1}{4} n Z |e| V_o A \tag{2.5}$$

(with A the collecting area, n, v_{the} the electron density and thermal velocity respectively). The function f, which depends from the electrode potential V, through

$$\phi^* = \left|\frac{eV}{kTe}\right| \left(\frac{\lambda_{de}}{R}\right)^{4/3} \tag{2.6}$$

(Te being electron temperature, λ_{de} the Debye radius and R the electrode's radius), is plotted in Fig. 1 and was derived by combining different models for particle attraction by large electrodes at large and moderate potentials (Alpert et al., 1965; Linson, 1969).

For the repelled particle contribution to the current, we used simply

$$\frac{i_j \text{ repelled}}{i_{jo}} = e^{-\left|\frac{eV}{kTe}\right|} \tag{2.7}$$

where V is now the repelling potential.

Approximate results for currents and potentials as a function of balloon radius, obtained with the above model for a perfectly conducting tether, are contained in (Anderson et al., 1979).

Recently, we have developed (Arnold and Dobrowolny, 1979) a more accurate method (based on a transmission line analogy of the tether system) to compute the stationary state described by (2.1) by solving a time dependent problem (and hence obtaining also the transient of the tether system towards the stationary state).

This method, which was especially devised for the more difficult case of computing current and potential distributions of a bare metallic tether, has now been applied to the tether - balloon system under consideration (conducting insulated tether with terminal electrodes), including also the effect of tether's resistance.

We give here in Fig. 2 the results obtained for the collection current I_c as a function of balloon radius r_b. The curve refers to a wire radius r_w = 0.5 mm, resistivity of the tether ρ = 0.15μΩm, length L = 100 km and an equivalent radius of the conducting part of the Shuttle of 1.78 m. It also applies to a configuration where the tether is moving perpendicularly to the magnetic field and is deployed downwards with respect to the Shuttle. Thus the Shuttle is at its nominal altitude of 220 km and the balloon at 120 km altitude.

From the curve we see that the limiting value of the current, determined by the tether's resistance R

$$i_R = \frac{V_o BL}{R} = 1.22 \text{ amps} \qquad (2.8)$$

is not yet reached at very large balloon dimensions (r_b > 50 m).

For a 5 meter radius balloon, one would get a collection current

$$I_c \sim 0.13 \text{ amps} \tag{2.9}$$

This value could of course be increased by the use of a suitable ion gun at the Shuttle.

Further results of this type of calculations (for different values of tether's resistance, and also for the configuration with the tether deployed upwards with respect to the Shuttle), will be obtained later on in this study.

The main purpose of presenting these results here is that of being able to compare them with values of the current parallel to magnetic field lines associated with waves radiated by the moving tether, as will be done in the following.

3. Discussion on possible waves radiated by the moving tether.

As the ionospheric conductivity parallel to the Earth's magnetic field, is extremely large, at altitudes above the E layer (and much larger than the transverse conductivity), the magnetic field lines can be regarded as equipotentials. The ionospheric state is perturbed by the motion of the tether (or any large conductor) across magnetic lines. From the rest frame of the plasma one sees a polarization electric field

$$\underline{E} = - \underline{V}_o \times \underline{B} \tag{3.1}$$

if we refer, for the moment, to the case of a perfectly conducting tether. A corresponding potential difference is therefore seen to be applied between the lines of force intercepted by the ends of the system.

This perturbed state tries to readjust itself (to the previous equilibrium state with no potential difference across field lines), through the propagation of waves from the region of disturbance. These waves (and associated currents parallel to $\underline{B}$ lines) are carrying away the applied potential differences or the equivalent transverse space charge.

The problem of wave radiation from the moving tether can be formally set up as a problem of radiation from a current source (i.e., the classical problem of antenna theory). For the case of interest to us, of radiation in a magnetized plasma, by combining Maxwell's equations and Fourier transforming in space and time, we obtain the following equation for the space-time Fourier transform of the radiated electric field

$$\Lambda_{ij}\ (\underline{k},\omega)\ E_j\ (\underline{k},\omega) = -\ \frac{4\pi i}{\omega}\ J_i^o \quad (\underline{k},\omega) \tag{3.2}$$

where ω, $\underline{k}$ are frequency and wavenumber of the radiated waves, $\underline{J}^o$ represents the current source (current density) and the tensor Λ_{ij} is defined by

$$\Lambda_{ij}\ (\underline{k},\omega) = n^2\ (x_i x_j - \delta_{ij}) - \varepsilon_{ij} \tag{3.3}$$

with

$$n = \frac{kc}{\omega} \tag{3.4}$$

the refractive index, $\underline{x} = \dfrac{\underline{k}}{|K|}$ and $\varepsilon_{ij}\ (\underline{k},\omega)$ being the dielectric tensor of the magnetized plasma. As it is well known (Stix, 1962)

$$\Lambda = \det \Lambda_{ij} = 0 \tag{3.5}$$

gives the wave dispersion relation.

The tether represents (for an observer at rest in the plasma) a moving current source so that we can write for the current density (considering motion in the y direction, see Fig. 3)

$$\underline{J}^0 = \underline{J}^0 (x, y - v_0 t, z) \tag{3.6}$$

Consequently, by Fourier transforming in space and time and substituting into eq. (3.1), we obtain

$$\Lambda_{ij} (\underline{k},\omega) E_j (\underline{k},\omega) = - \frac{i}{\omega} \delta (\omega - k_y v_0) J_i^0 (\underline{k}) \tag{3.7}$$

The purpose of writing this equation is to point out that it gives a constraint on the frequency of the radiated waves, which must satisfy

$$\omega = k_y v_0 \tag{3.8}$$

This does not of course fix the frequency which depends from k_y, which, in turn, depends from the function $\underline{J}^0 (\underline{k})$ and from the role played by the plasma dispersion in the solution of (3.7).

It is quite natural to estimate

$$k_y \sim \frac{1}{d_y} \tag{3.9}$$

where d_y is the conductor's dimension in the direction of motion. This then gives a frequency

$$\omega^* = \frac{V_0}{d_y} \tag{3.10}$$

It is important, however, to realize that this is not necessarily a typical frequency of the radiated waves, but rather must be interpreted as an upper limit to the radiated frequencies. In other words one can say that the power radiated in frequencies $\omega >> \omega^*$ will be certainly negligible. On the other hand, all frequencies

$$\omega \lesssim \omega^* \tag{3.11}$$

can in principle be radiated, but, of course, a formal calculation of power $P(\omega)$ as a function of frequency is necessary to ascertain how and if the efficiency of the generator varies with frequency.

If we impose the condition

$$\omega^* < \Omega_{ci} \tag{3.12}$$

(Ω_{ci}, being the ion gyrofrequency, $\Omega_{ci} \sim 200$ Hz at the altitudes of interest), which gives, for our parameters

$$d_y > d_y^* = \frac{V_o}{\Omega_{ci}} \sim 40 \text{ meters}, \tag{3.13}$$

we are imposing the condition that all the waves generated fall in the hydromagnetic range (Alfvèn waves) and, hence, that all the power available for wave generation goes into these low frequency waves.

On the other hand, if

$$d_y < d_y^* \tag{3.14}$$

this does not mean that low frequency Alfvèn waves are not generated but rather that the power radiated will not only go in Alfvèn but also in higher frequency waves (whistlers, for example).

These statements require of course that the space Fourier transform of the current $\underline{J}^o$ $(\underline{k})$, as a function of k_y, will not be peaked around a certain value of k_y different from zero. This is however ensured for distributions of currents which are limited in space, like in the case of the tether, in which case the k_y distribution of current will be actually peaked around $k_y = 0$.

With the above observations in mind, we can now discuss which waves can be in principle irradiated by the tether-balloon system. Here, we have two different dimensions parallel to the direction of motion, namely, the tether's diameter

$$d_w = 1 \text{ mm} \tag{3.15}$$

and the balloon diameter $2r_b$ (for simplicity we suppose, in the following discussion, to have two equal balloons at the termination of the tether, see Fig. 3). Correspondingly we have two frequencies

$$\omega^*_{tether} \sim \frac{V_o}{d_w} \sin\alpha \sim 7.8 \times 10^6 \sin\alpha \text{ Hz} \qquad (3.16)$$

$$\omega^*_{balloon} \sim \frac{V_o}{2r_b} \sin\alpha \qquad (3.17)$$

wehre we have added the factor $\sin\alpha$ (with α the angle between $\underline{V}_o$ and $\underline{B}$) to account for any direction of motion of the tether with respect to the Earth's magnetic field. The first frequency is a very high one (in the earth's ionosphere, between 100 and 300 km, the electron plasma frequency ω_{pe} varies between 5 and 10 MHz and the electron gyrofrequency $\Omega_{ce} \sim 1$ MHz). The balloon frequency, taking for example $r_b = 5$ m, would be

$$\omega^*_{balloon} \sim 780 \sin\alpha \text{ Hz}$$

and would fall in the lower range of whistler waves (close to the ion gyrofrequency $\Omega_{ci} \sim 200$ Hz). On the other hand, as it follows from (3.13), a balloon radius

$$r_b > 20 \text{ meters}$$

would be necessary (for motion perpendicular to $\underline{B}$) to have $\omega^*_{balloon}$ falling already in the hydromagnetic range.

The conclusion is that we might in principle expect a very wide range of frequencies (from around the electron cyclotron frequency to essentially zero), and therefore, both whistlers and hydromagnetic waves, to be radiated from the moving tether. The problem is thus, in this respect, more complex than in the case of the moon of Jupiter Io, where dimensions are such ($d_{Io} = 3640$ km) that the frequency ω^*, defined by (3.10), falls

already in the Alfvènic range ($\omega^*_{Io} \sim 0.015$ Hz) and hence the electromotive power available (or better that part which goes into waves) does go into Alfvèn waves only.

4. Parallel current associated with Alfvèn waves.

The coupling of the tether's system with the plasma medium and, possibly, with the lower layers of the ionosphere, occurs through the radiation of waves. In particular, if a current $J_{||}$, parallel to magnetic field lines, is associated with these waves, it is this current which continues the tether current into the ionosphere, down to E layer altitudes where perpendicular current closure can take place.

It is this parallel wave current which is beyond the so called "dc current model" of Io, early proposed by Goldreich and Linden Bell (1969). According to this, the flux tube intercepted by Io would be actually frozen to the satellite and follow its motion around Jupiter, with upgoing and downgoing parallel currents at the boundaries of the tube (the Alfvènic currents) and circuit closure, within Io, on one side, and across Jupiter's ionosphere, on the other side.

We will now derive a general equation (with no approximation of small amplitude for the waves) for the parallel current associated with Alfvèn waves and then estimate from that the magnitude of this current for the tether balloon systems. We recall, first of all, that the Alfvèn wave characteristics are given by (Jeffrey and Taniuti, 1964)

$$\underline{V} \pm \frac{\underline{B}}{(\mu_0 \rho)^{1/2}} = \text{constant} \qquad (4.1)$$

where $\underline{V}$, $\underline{B}$ refer to the fluctuations of velocity and magnetic field in the waves and ρ is the plasma mass density. The constant can be evaluated

from the background properties of the plasma. In the rest frame of the plasma, then

$$\underline{V} \pm \frac{\underline{B}}{(\mu_o \rho)^{1/2}} = \underline{V}_A = \frac{\underline{B}_o}{(\mu_o \rho)^{1/2}} \tag{4.2}$$

with $\underline{B}_o$ the earth's magnetic field.

For infinite conductivity along magnetic lines, we have

$$E_{||} = 0 \tag{4.3}$$

and Ohm's law reduces to

$$\underline{E}_{\underline{|}} + \underline{v} + \underline{B} = 0 \tag{4.4}$$

Taking now the divergence of this equation and combining with (4.2), it is easy to arrive at

$$\nabla_{\underline{|}} \cdot \underline{E}_{\underline{|}} = \mu_o V_A J_{||} \tag{4.5}$$

which relates the space charge (or potential difference) across field lines (which in our problem corresponds to the electromotive force applied by the tether between different field lines) with the parallel current associated with the waves.

On the other hand, by combining Maxwell's equations

$$\nabla \times \underline{E} = - \frac{\partial \underline{B}}{\partial t}$$

$$\nabla \times \underline{B} = \mu_o \underline{J}$$

we arrive at

$$\nabla \nabla \cdot \underline{E} - \nabla^2 E = \mu_o \frac{\partial \underline{J}}{\partial t} \tag{4.6}$$

and, projecting along the magnetic field (z) direction, and taking (4.3) into account,

$$\frac{\partial}{\partial z}\,(\nabla_{\perp}\cdot\underline{E}_{\perp}) = \mu_o \frac{\partial J_z}{\partial t} \quad . \tag{4.7}$$

Combining (4.7) with (4.5), we can write, for example,

$$\frac{\partial}{\partial t}\,(\nabla_{\perp}\cdot\underline{E}_{\perp}) = V_A \frac{\partial}{\partial z}\,(\nabla_{\perp}\cdot\underline{E}_{\perp}) \tag{4.8}$$

which tells us that the transverse space charge propagates, within the MDH framework, parallel to magnetic field lines, at the Alfvèn speed.

Eq. (4.5) can now be used to calculate the parallel current for the tether-balloon system. As the tether itself is covered by an insulator, the outside current flows only along the flux tubes intercepted by the balloon and the Shuttle(*). Then, referring to the case of two equal balloons at the ends (see Fig. 3), and supposing the current uniformly distributed across each flux tube (which corresponds to the idea of an homogeneous particle collection by the balloon along the lines of force), we have

$$J_{||} = \frac{I_{Aw}}{\pi r_b^{\,2}} \tag{4.9}$$

Then, from eq. (4.5)

$$I_{Aw} \sim \frac{\pi}{2}\, r_b\, \frac{1}{\mu_o V_A}\, E_{\perp} \tag{4.10}$$

The perpendicular electric field, taking ohmic losses in the tether into account, is given by

$$E_{\perp} = E_{\perp o} - \frac{R_w I_{Aw}}{L} \tag{4.11}$$

where $E_{\perp o}$ is the total Lorentz field and (for motion perpendicular to $\underline{B}$)

(*) actually, the Alfvènic current flows at an angle θ_A with respect to field lines given by $\theta_A = \arctan \frac{V_o}{V_A}$. In our case this is, typically, $\theta_A \sim 0.55°$ and is not important for the following estimates.

$$E_{\underline{I}o} = V_o B = 0.23 \text{ volt/m} \tag{4.12}$$

R_W is the tether's resistance and L is its length. Thus we can write

$$I_{Aw} = \frac{Io}{1 + \frac{\pi}{2}\frac{r_b}{L}\frac{R_W}{\mu_o V_A}} \tag{4.13}$$

where

$$I_o = \frac{\pi}{2} r_b \frac{1}{\mu_o V_A} E_{\underline{I}o} \tag{4.14}$$

is the total parallel current in Alfven waves which one would have for a perfectly conducting tether.

Fig. 4 reproduces the Alfvènic current I_{Aw} as a function of balloon radius for a steel tether (resistivity $\rho = 0.15$ μΩm), of length L = 100 km and having taken $V_A \sim 800$ km/sec as an average value for the Alfvèn speed between 100 and 300 km of altitude.

We see that the resistive limit to the current, $i_R = 1.22$ amps [see (2.8)] is not yet reached at quite high values of the balloon radius (r_b=50m).

From the curve we derive that, for example, for a balloon radius r_b = 5 m, the Alfvènic current is

$$I_{Aw} \sim 0.725 \text{ amps}$$

5. Power and impedance associated with Alfvèn waves.

An estimate of the power associated wtih Alfvèn waves can be obtained by multiplying the wave energy density W for the volume filled up by the wave energy in a second. This, in turn will be equal to the wave group velocity V_G multiplied by the cross section of the flux tubes intersected by the tether balloon system.

Hence,

$$P \sim W \times 2\ (2\pi r_b^2 + Ld_w)V_G \tag{5.1}$$

In the bracket, the two different contributions correspond to the tether cross section and the two balloon cross sections. The factor 2 corresponds to the fact that we have wave propagation in two opposite directions with respect to the tether system (down to conjugat. regions of the low ionosphere). The general expression for the energy density of waves in a magnetized plasma is (Stix, 1962)

$$W = \frac{1}{4\mu_o}\left(|B^2| + E_i \frac{\partial}{\partial\omega}(\omega\varepsilon_{ij})\, E_j\right) \tag{5.2}$$

with $\varepsilon_{ij}\ (\underline{k},\omega)$ the plasma dielectric tensor.

For Alfvèn waves, it is easy to show that

$$W_{Aw} = \frac{B^2}{2\mu_o} \tag{5.3}$$

<u>i.e.</u>, the energy of the fluctuations is entirely magnetic. Thus, using also $V_G = V_A$, we obtain for the power P_{Aw} associated with Alfvèn waves

$$P_{Aw} \sim \frac{B^2}{\mu_o} V_A\ (2\pi r_b^2 + Ld_w) \tag{5.4}$$

From Maxwell's equation, in order of magnitude,

$$B \sim \frac{1}{V_A} E_{\underline{l}} \tag{5.5}$$

Thus, in terms of the transverse electric field

$$P_{Aw} \sim \frac{E_{\underline{l}}^2}{\mu_o V_A}\quad (2\pi r_b^2 + Ld_w) \tag{5.6}$$

The Alfvèn velocity, between 100 and 300 km varies, on account of the plasma density variation, between 1070 and 520 km/sec. In the numerical estimates, we will use an average value

$$V_A \sim 800 \text{ km/sec}$$

Thus, as a numerical example, for

$$r_b = 5\text{m},\ d_w = 10^{-3}\text{m},\ L = 10^5\text{m},\ \rho = 0.15\ \mu\Omega\text{m},$$

using $\underline{E_l} = \underline{E_{lo}} - \frac{R_w I_{Aw}}{L}$ and the results of Fig. 4 for the Alfvènic current we obtain

$$P_{Aw} \sim 10 \text{ watts}$$

One must be cautioned at this point that this number has nothing to do with the power in Alfvèn waves detectable at ground. The previous estimate gives us only the power within the cross section of the flux tubes intersected by the system. The problem of transmission, through the Earth's atmosphere, down at ground has not been touched at this time, but we might reasonably suppose to have a large spreading of the waves in the low atmosphere. Thus (taking also into account that the transit time of Alfvèn waves from the tether to the E layer is a fraction of a second), at ground we will not collect just the power corresponding to the cross section of the tether system, but, as the tether is moving (and it covers 7.8 km in 1 sec), rather the cumulative effect of the Alfvènic emission over a certain distance covered by the tether. This may mean a great increase with respect to the value obtained by (5.6). This point will be further elaborated in the continuation of this work. An input impedance of the balloon flux tubes can now easily be obtained from

$$Z_{Aw} = \frac{\Delta V}{I_{Aw}} \tag{5.7}$$

where

$$\Delta V = 2r_b E_{\perp} \tag{5.8}$$

is the potential difference across the flux tube. Using (4.10) for the current, we obtain

$$Z_{Aw} = \frac{4}{\pi} \mu_o V_A \tag{5.9}$$

An average value, for the altitudes of interest is

$$Z_{Aw} \sim 1.3 \text{ ohms}$$

6. Comparison of Alfvènic current with current due to charged particle collection.

In Fig. 5 we have plotted, as a function of balloon radius, both the current I_c obtained from charged particle collection at the end electrodes of the tether (see Sect. 2) and the current I_{Aw} along the balloon flux tube associated with Alfvèn waves (see Sect. 4).

The curves refer to a tether with L = 100 km, ρ = 0.15 $\mu\Omega$m and the configuration with the Shuttle at h = 220 km and the balloon deployed downward.

The next graph (Fig. 6), gives the ratio I_c/I_{Aw} as a function of r_b. It is seen that the Alfvènic current is always greater than the collection current, the two curves approaching only for very high values of the balloon radius (r_b > 50 meters).

On the assumption that the current in the tether system has to be carried away (along magnetic flux tubes) through Alfvèn waves, the results

of Figs. 5 and 6, indicate that it is particle collection at the electrodes which determines the value of the current in the system. In other words, the current in the Alfvèn wings (or, approximately, the flux tubes intercepted by the balloon and the Shuttle) is limited to the value I_c, at least for reasonable balloon dimensions.

Further results of this comparison, for different tether resistance and for the configuration with the balloon upward, will be obtained in the next phase of this study.

7. Reconsideration of power associated with Alfvèn waves.

The fact that

$$I_c < I_{Aw} \tag{7.1}$$

leads to a re-estimation of the power associated with Alfvèn waves radiated by the tether.

Considering the current as limited by particle collection and given by the value I_c, and going back to formula (4.10), we see that now we must say that the transverse electric field $E_\perp'$ transported by the waves is reduced (with respect to the previously considered value $E_\perp$, given by 4.11), by a factor I_c/I_{Aw}, i.e.,

$$E_\perp' = \frac{I_c}{I_{Aw}} E_\perp \tag{7.2}$$

The power, given by (5.6), will be correspondingly reduced by a factor $(I_c/I_{Aw})^2$

$$P_{Aw} = \frac{1}{\mu_o V_A} E_\perp^2 (2\pi r_b^2 + L d_w) \left(\frac{I_c}{I_{Aw}}\right)^2 \tag{7.3}$$

Using again (4.10), we obtain

$$P_{Aw} = \frac{4}{\pi^2}\ \mu_o V_A\ (2\pi + \frac{Ld_w}{r_b^2})\ \ I_c^2 \qquad (7.4)$$

8. Physical picture of the Alfvèn wave system associated with the tether.

When the Alfven waves radiated by the tether system reach the E layer of the ionosphere, they find a change in transverse conductivity. The corresponding parallel current system then closes transversally to the magnetic field through Pedersen and Hall conductivities. A result of the reaction of the dense ionospheric layer to the electric field of the wave is then, first of all, a partial reflection of the wave electric field.

We can write

$$\underline{E}_{\perp}^{up} = R\ \underline{E}_{\perp}^{down} \qquad (8.1)$$

where $\underline{E}_{\perp}^{down}$ is the transverse electric field of the downgoing wave, $\underline{E}_{\perp}^{up}$ the electric field of the reflected wave and the reflection coefficient R, is found to be given (Mallinckrodt and Carlson, 1978) by

$$R = \frac{1 - X}{1 + X} \qquad (8.2)$$

with

$$X = \frac{\Sigma_p}{\Sigma_{Aw}} = \frac{4}{\pi}\ \mu_o V_A\ \Sigma_p \qquad (8.3)$$

being the ratio between the Pedersen integrated conductivity Σ_p and the Alfvèn wave conductivity ($\Sigma_{Aw} = 1/Z_{Aw}$).

If $X \gg 1$, the electric field (and therefore the $\underline{E}_1 \times \underline{B}$ plasma velocity) at the boundary, is zero. The E layer of the ionosphere acts in this case as a metallic boundary with frozen in magnetic lines. On the contrary, if $X \ll 1$, we obtain at the boundary twice the amplitude of the incoming wave. This case means negligible conductivity of the ionospheric E layer so that (in the limit of a perfectly insulating E layer) the magnetic lines have no further identity in this region.

To obtain numerical values for the reflection coefficient we take as typical values for Σ_p (Hanson, 1965)

$$\Sigma_p \sim \begin{cases} 10 \text{ mhos} & \text{at day time} \\ 3 \times 10^{-2} \text{ mhos} & \text{at night time} \end{cases} \tag{8.4}$$

Taking an average E layer altitude of h = 100 km, we can further use the following values of electron density

$$n_e \sim \begin{cases} 2 \times 10^5 \text{ cm}^{-3} & \text{at day time} \\ 2 \times 10^3 \text{ cm}^{-3} & \text{at night time} \end{cases} \tag{8.5}$$

to determine the Alfvèn speed at the E layer. The final typical results for the reflection coefficient R, are

$$R \sim \begin{cases} -0.92 & \text{at day time} \\ +0.17 & \text{at night time} \end{cases} \tag{8.6}$$

We thus see that, whereas there is almost complete reflection from the day time ionosphere, reflection is quite weak from the night side.

The next point to consider is the propagation time of Alfvèn waves from the tether system to the E layer levels. This varies of course from one end to the other of the tether causing reflection (or partial reflection)

of different parts of the wave front at different times.

Taking a typical distance of 100 km and an average Alfvèn speed of 800 km/s, would however give a round trip time of the Alfvèn wave of

$$\tau \sim 0.25 \text{ sec}$$

in which time the tether balloon system has moved by a distance

$$\Delta y \sim 2 \text{ km}$$

Clearly, therefore, the reflected waves will not find any more the tether-balloon system on their way back from the E layer. Thus, an influence of the ionospheric E layer on the current in the tether system, like it was indicated in the case of the moon of Jupiter Io (Goldreich and Linden-Bell, 1969), is not possible.

The picture of a so called "dc current circuit" moving with the tether, i.e., a freezing with the tether's motion of the intercepted flux tubes (which would then slip with respect to the ionospheric base), is therefore not appropriate.

What happens is that the Alfvèn waves radiated by the tether are partially reflected from the ionospheric E layer and then travel back to the conjugate ionosphere where they are again partially reflected, and so on. The tether system during its motion generates therefore a system of waves reflected back and forth between conjugate zones of the E layer, all along its orbit.

It is interesting to ask how many reflections are possible before a given wave decreases significantly in amplitude. When reflections are occurring with the same reflection coefficient R, the number of successive

reflections necessary to have a $\frac{1}{e}$ reduction of the wave amplitude, would be

$$N \sim \frac{\Sigma_p}{2\Sigma_A} \left(1 + \frac{1}{e}\right) \quad \text{for } \Sigma_p > \Sigma_A \tag{8.7}$$

Thus, $N \sim 12$ for reflections between day time ionospheres, whereas, in the case of night time ionospheres ($R \sim 0.17$) the wave amplitude is already drastically reduced at the first reflection.

The next point we will have to examine i. transmission of the Alfvèn waves from the E layer to the ground. Considerations on this will be one of the objects of the next part of this work.

9. Power, current and impedance for parallel electron whistler waves.

As mentioned in Sect. 3, the tether irradiates in principle waves from high to very low frequencies and, hence, besides the Alfvèn waves considered so far, also whistler waves.

It is then of interest to calculate, in the same way we have done for Alfvèn waves, the power irradiated in whistler waves, the parallel current associated with these waves and the corresponding input impedance.

We do that for the simpler case of whistler waves propagating parallel to magnetic field lines. Although the tether can in principle radiate whistler waves propagating at a range of angles with respect to the magnetic field, the group velocity of electron whistlers, although depending from the angle of propagation with respect to the magnetic field, is never greater than $\sim 20°$ (Helliwell, 1965). Hence the parallel case should be a significant one.

In the parallel case, the index of refraction of the waves is given by

$$n^2 = 1 - \frac{\omega_{pe}^2}{\omega(\omega - \Omega_{ce})} \tag{9.1}$$

(at least neglecting the ion motion, which is valid for frequencies not too close to the ion cyclotron frequency $\Omega_{ci} \sim 200$ Hz).

It can be seen that, for parallel propagation, the group velocity V_G is related to the phase velocity V_p by

$$V_G = 2V_p \left(1 - \frac{\omega}{\Omega_{ce}}\right) \tag{9.2}$$

Fig. 7 gives curves of the group velocity and phase velocity (both normalized to the speed of light c), versus ω/Ω_{ce}, for $\frac{\omega_{pe}^2}{\Omega_{ce}^2} \sim 10^2$, which is appropriate to the ionospheric altitudes of interest to us.

The energy density of the waves must be computed from (5.2) where, using Stix's notation (Stix, 1962) the dielectric tensor ε_{ij} is given by

$$\varepsilon_{ij} = \begin{pmatrix} S & -iD & 0 \\ iD & S & 0 \\ 0 & 0 & P \end{pmatrix}$$

$$S = \frac{1}{2}(R+L),\ D = \frac{1}{2}(R-L),\ P = 1 - \frac{\omega_{pe}^2}{\omega^2}$$

$$R \sim 1 - \frac{\omega_{pe}^2}{\omega(\omega-\Omega_{ce})},\quad L \sim 1 - \frac{\omega_{pe}^2}{\omega(\omega+\Omega_{ce})}$$

The result we obtain from (5.2) is then

$$W = \frac{1}{2\mu_o}\left(1 + \frac{\omega}{\Omega_{ce}}\right) B^2 \tag{9.3}$$

The power P_{ww} in parallel whistler waves, will therefore be given by

$$P_{ww} = \frac{1}{\mu_o}\left(1 + \frac{\omega}{\Omega e}\right)\ B^2\ V_g\ (2\pi r_b^2 + Ld_w) \tag{9.4}$$

and, in terms of the transverse electric field,

$$P_{ww} \sim \frac{E_{\perp}^2}{\mu_o} \left(1 + \frac{\omega}{\Omega_{ce}}\right) \frac{V_G}{V_p}^2 \left(2\pi r_b^2 + L d_w\right) \tag{9.5}$$

Using the relation (9.2), we finally obtain

$$P_{ww} = \frac{2}{\mu_o} \left(1 - \frac{\omega^2}{\Omega_{ce}}^2\right) \left(2\pi r_b^2 + L d_w\right) \frac{E_{\perp}^2}{V_p} \tag{9.6}$$

The current, which will be carried away along the flux tubes intercepted by the end electrodes (which we take again as balloons of radius r_b) is

$$I_{ww} \sim \frac{\pi}{\mu_o} r_b \left(1 - \frac{\omega^2}{\Omega_{ce}}^2\right) \frac{E_{\perp}}{V_p} \tag{9.7}$$

The corresponding impedance

$$Z_{ww} = 2 \frac{\mu_o}{\pi} V_p \left(1 - \frac{\omega^2}{\Omega_{ce}}^2\right)^{-1} \tag{9.8}$$

10. Comparison between Alfvèn waves and whistler wave impedance.

It is important to compare the impedance associated with Alfvèn waves transmission from the tether with the corresponding impedance for whistler waves. From (5.9) and (9.8) we obtain

$$\frac{Z_{ww}}{Z_{aw}} = \frac{1}{2} \frac{V_p}{V_A} \left(1 - \frac{\omega^2}{\Omega_{ce}}^2\right)^{-1} \tag{10.1}$$

This ratio has been plotted in Fig. 8 as a function of $\frac{\omega}{\Omega_{ce}}$. It is seen that, except at low frequencies (close to the ion cyclotron frequency) this ratio is always greater than unity.

The interpretation of this is that, for equally applied potentials (across the flux tubes), much more current (and hence power) would go in low frequency Alfvèn waves than in whistler waves. The ratio between the two powers (for equal $E_{\perp}$) is in fact given by

$$\frac{P_{Aw}}{P_{ww}} \sim \frac{Z_{ww}}{Z_{Aw}} >> 1 \qquad (10.2)$$

Although a more definite conclusion would need to be based on a calculation of the frequency dependence of the power radiated by the tether as a current source, this is a strong indication towards the attitude of the system to radiate low frequency Alfvèn waves more than higher frequency waves.

11. Conclusions and comments on future developments.

We end up with some comments on problems to be considered in the remaining part of this study. A problem, which we did not touch in this intermediate report, is that of the possible generation from the tether system of beams of high energy electrons accelerated towards the Earth's atmosphere. This possibility arises in a configuration with the tether deployed downwards, with a sufficiently large potential drop between the balloon and the plasma, on account of secondary electrons generated by the impact of ionospheric ions at the balloon's surface (Dobrowolny et al., 1979). The secondary electrons find a sheath potential drop of the right polarity to be accelerated down to the Earth along magnetic lines of force.

We plan to include this effect in the calculation of the current in the tether (and potentials of the end electrodes with respect to the plasma). Some considerations on the velocity distributions of such accelerated

electrons and the possible instabilities they can excite, will also be developed. More important, at this stage, will be to decide what fraction of the electromotive energy, originating from the motion of the conducting tether, goes into these accelerated beams, and which goes into waves.

As far as the waves are concerned, either Alfvèn or whistler waves, we will have to discuss what power must be expected at ground. This implies consideration of propagation from E layer down to Earth's surface and screening effects of the Earth's atmosphere.

12. References

Alpert Ya.L., Gurevich A.V., and Pitaevskii L.P., 1965. Space Physics with artificial satellites. Consultant Bureau, New York.

Anderson M.P., Arnold D.A., Colombo G., Dobrowolny M., Grossi M.D., and Kirschner L.R., 1979. "Orbiting tether's electrodynamic interactions." Final Report, NASA Contract NAS5-25077, April 1979.

Arnold D.A. and Dobrowolny M., 1979. Transmission line model of the interaction of a long metal wire with the ionosphere. Harvard-Smithsonian Center for Astrophysics Preprint Series No. 1178; to be published in Radio Science, 1980.

Dobrowolny M., Colombo G., and Grossi M.D., 1976. "Electrodynamics of long tethers in the near-Earth environment." SAO Report in Geoastronomy, No. 3, October 1976; reissued April, 1979.

Dobrowolny M., Arnold D.A., Colombo G., and Grossi M.D., 1979. Mechanisms of electrodynamic interactions between a tethered satellite system and the ionosphere. SAO Reports in Radio and Geoastronomy, No. 6, August 1979.

Goldreich P. and Lynden-Bell D., 1969. Io, a Jovian unipolar inductor. Astrophys. Jour. vol. 156, pp. 59-78.

Hanson W.B., 1965. Structure of the ionosphere. In: Satellite Environment Handbook, ed. by F.S. Johnson, Stanford Univ. Press, Stanford, CA, pp. 23-41.

Helliwell R.A., 1965. Whistlers and related ionospheric phenomena. Stanford Univ. Press, Stanford, CA.

Jeffrey A. and Taniuti T., 1964. Non linear wave propagation. Academic Press, New York.

Kalaghan P.M., Arnold D.A., Colombo G., Grossi M.D., Kirschner L.R., and Orringer O., 1978. "Study of the dynamics of a tethered satellite system (Skyhook). Final Report, NASA Contract NAS8-32199, March 1978.

Linson L.M., 1969. Current-voltage characteristics of an electron-emitting satellite in the ionosphere. Journ. Geophys. Res. vol. 74, pp. 2368-2375.

Mallinckrodt A.J. and Carlson C.W., 1978. Relations between transverse electric fields and field aligned currents. Journ. Geophys. Res. vol. 83, pp. 1426-1432.

Stix T.H., 1962. The Theory of Plasma Waves. McGraw Hill Company.

Figure Captions

Figure 1. Graph of the function $f(\phi^*)$.

Figure 2. Collection current I_c versus balloon radius r_b.

Figure 3. Geometry of the tether-balloon system.

Figure 4. Alfvènic current I_{Aw} versus balloon radius r_b.

Figure 5. Collection (I_c) and Alfvenic (I_{Aw}) currents versus balloon radius.

Figure 6. Ratio between collection (I_c) and Alfvènic (I_{Aw}) currents versus balloon radius r_b.

Figure 7. Phase (V_p) and group (V_G) velocities for parallel electron whistlers versus ω/Ω_{ce}.

Figure 8. Ratio of whistler (Z_{ww}) to Alfvèn wave (Z_{Aw}) impedance, versus normalized frequency ω/Ω_{ce}.

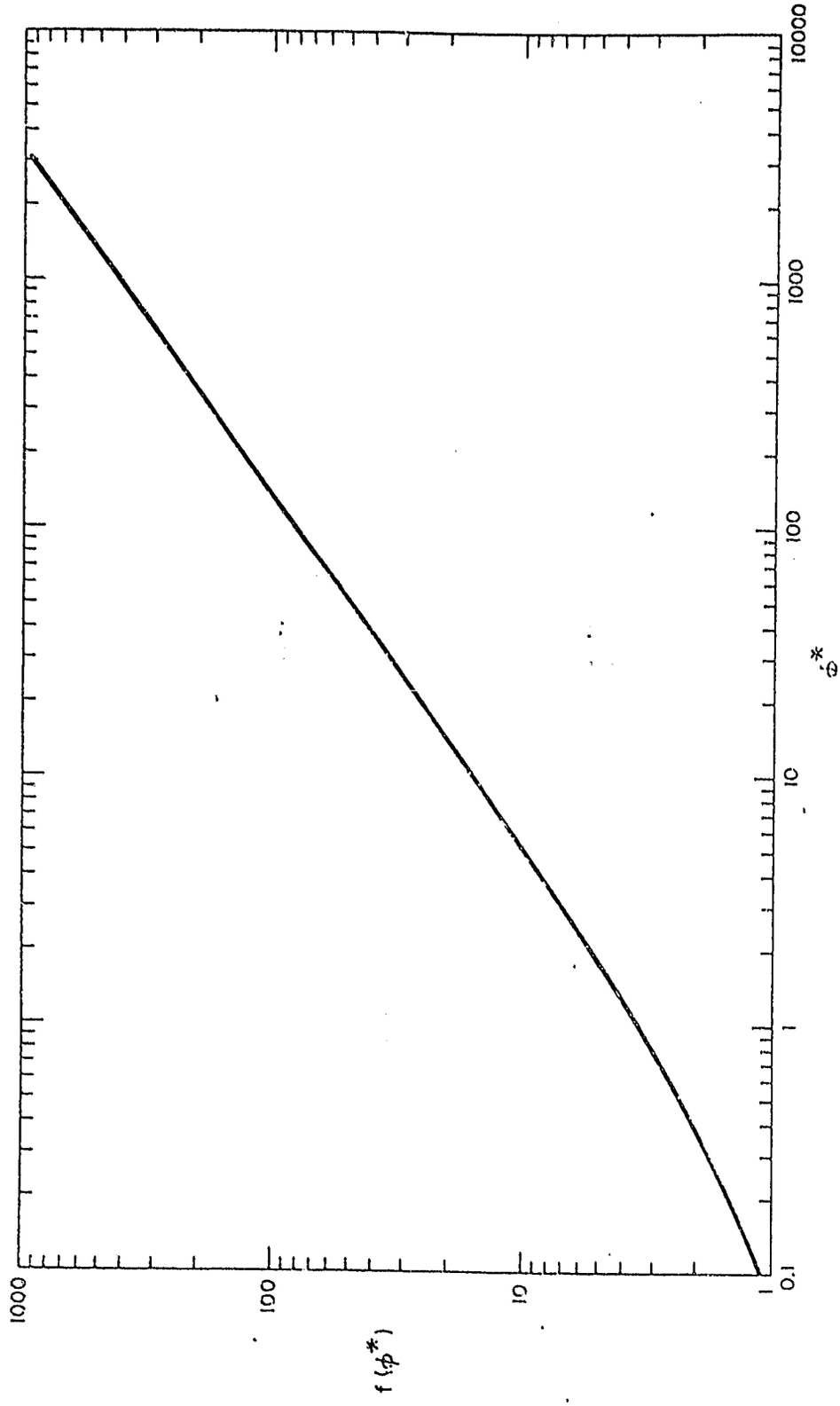

Figure 1. Graph of the function $f(\phi^*)$.

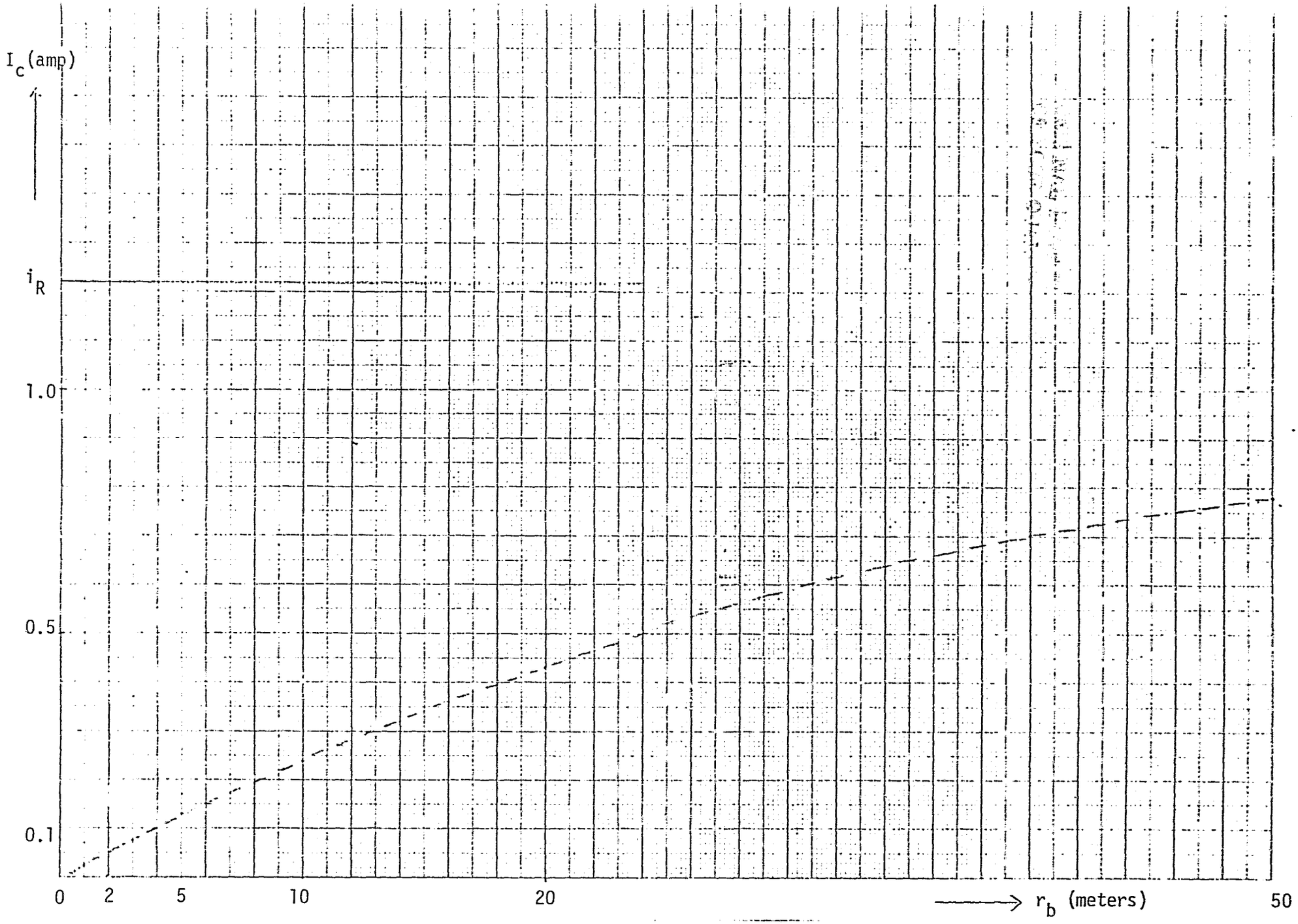

Figure 2. Collection current I_c versus balloon radius r_b.

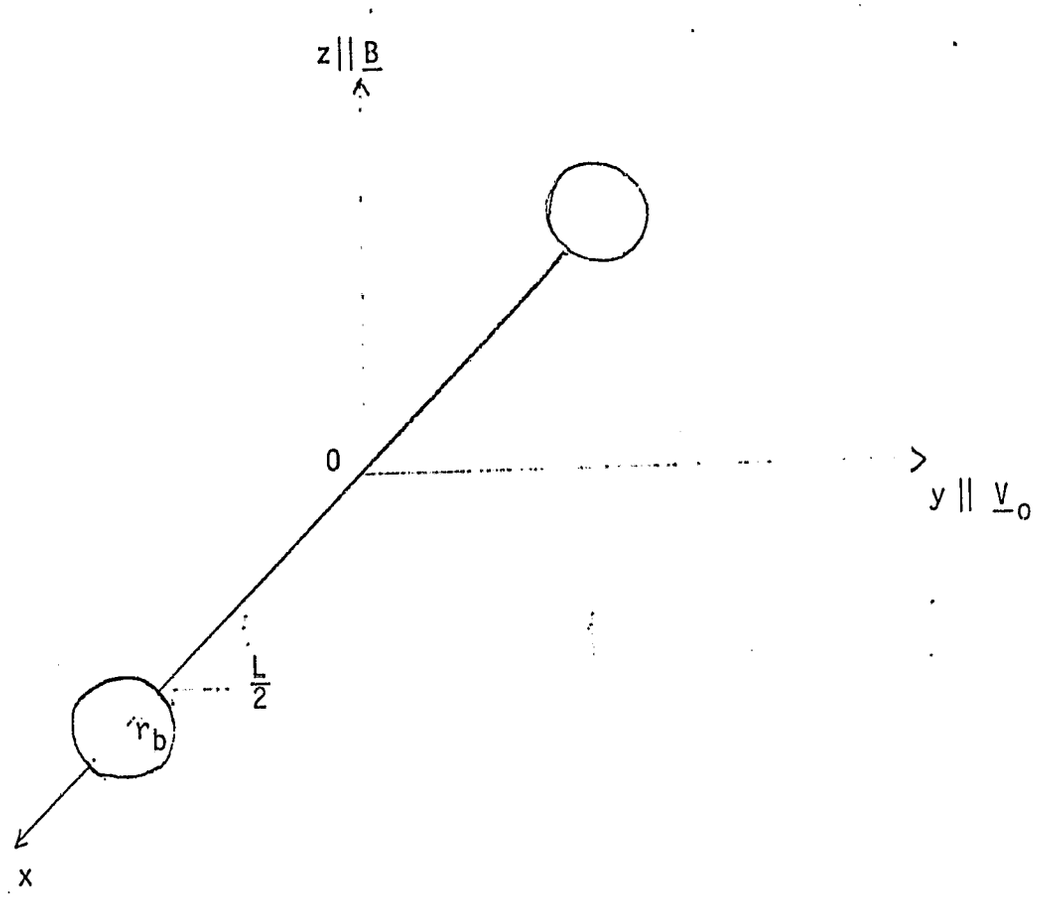

Figure 3. Geometry of the tether-balloon system.

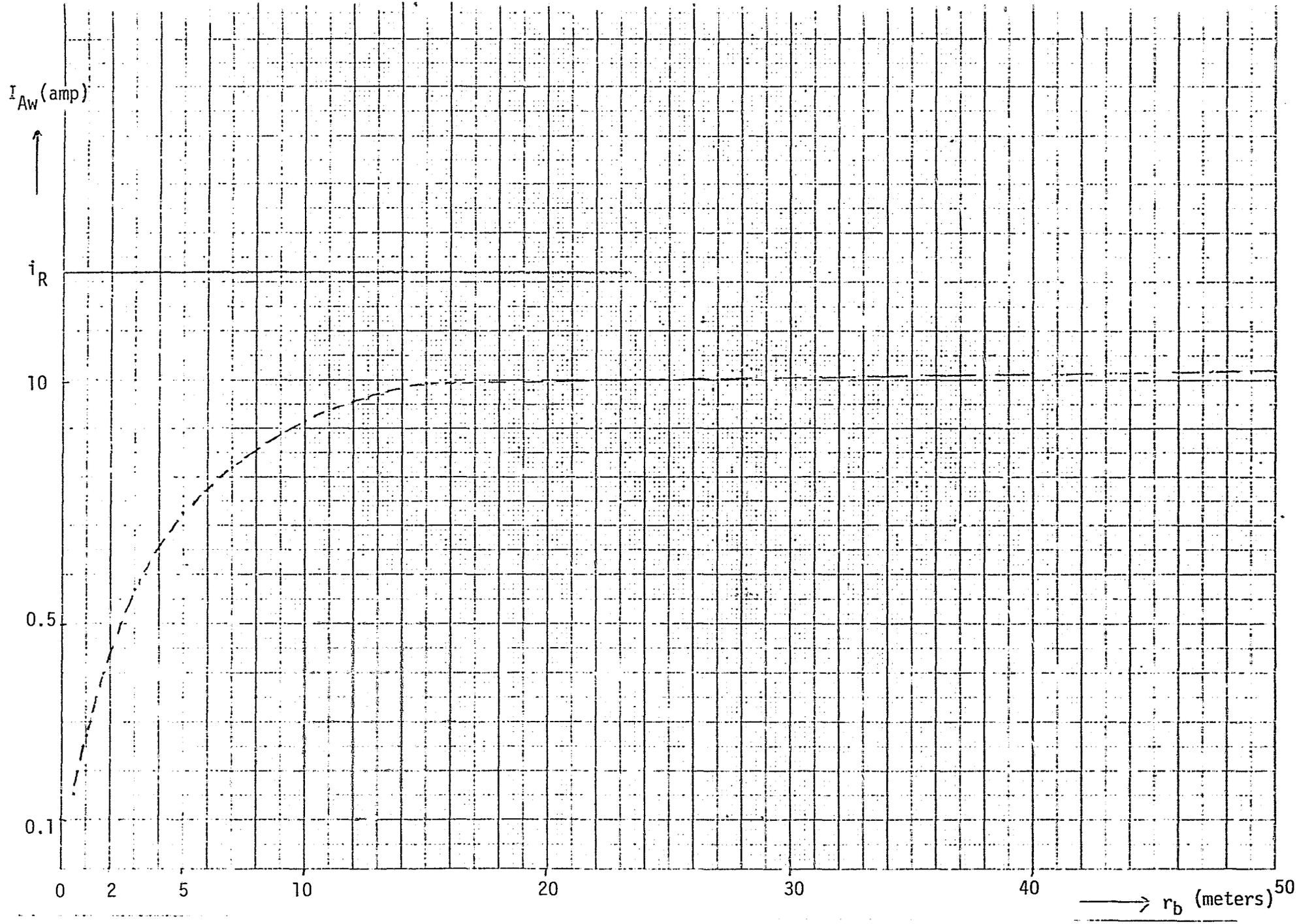

Figure 4. Alfvènic current I_{Aw} versus balloon radius r_b.

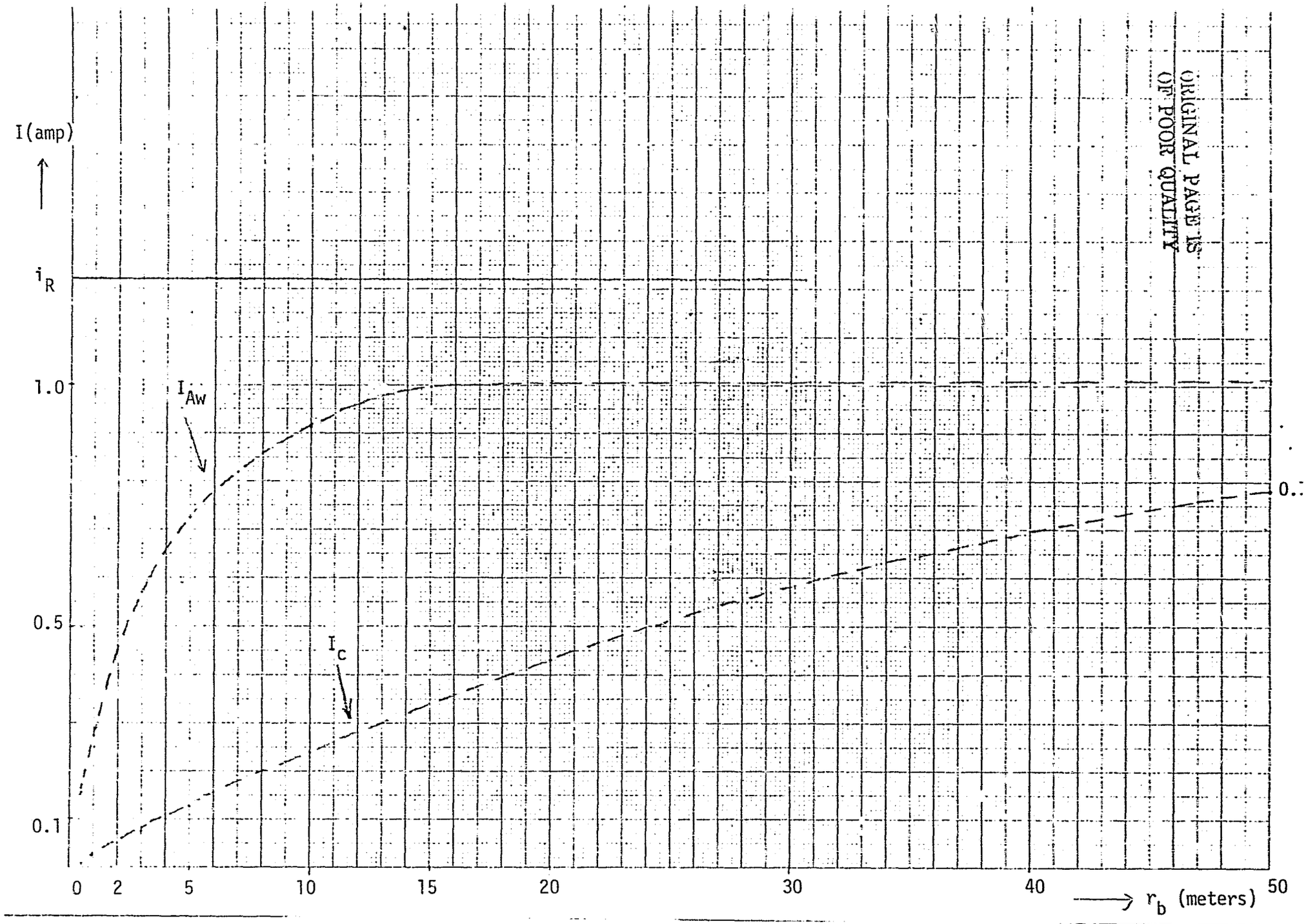

Figure 5. Collection (I_c) and Alfvènic (I_{Aw}) currents versus balloon radius.

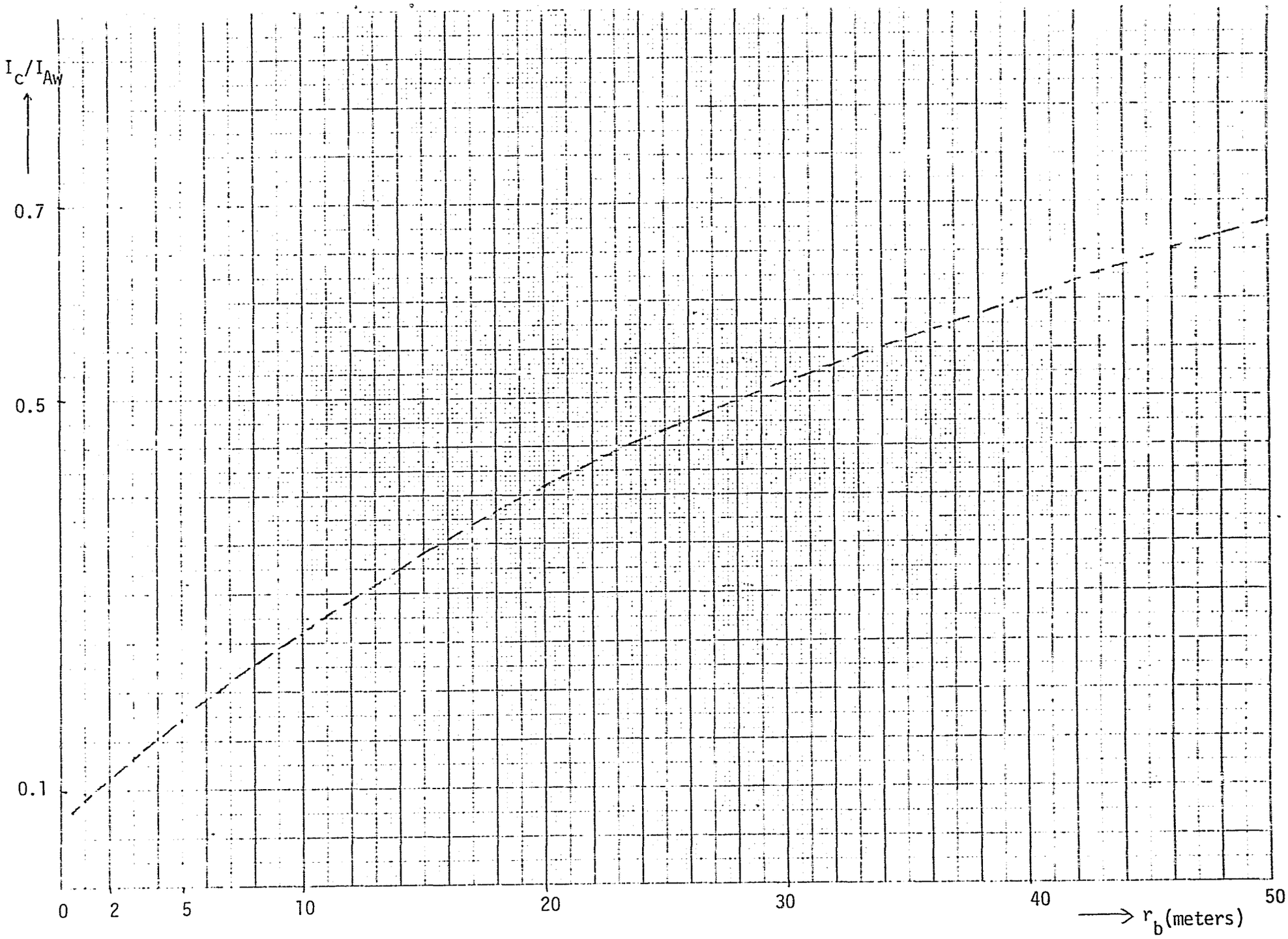

Figure 6. Ratio between collection (I_c) and Alfvènic (I_{Aw}) currents versus balloon radius r_b.

Figure 7. Phase (v_p) and group (v_G) velocities for parallel electron whistlers versus ω/Ω_{ce}.

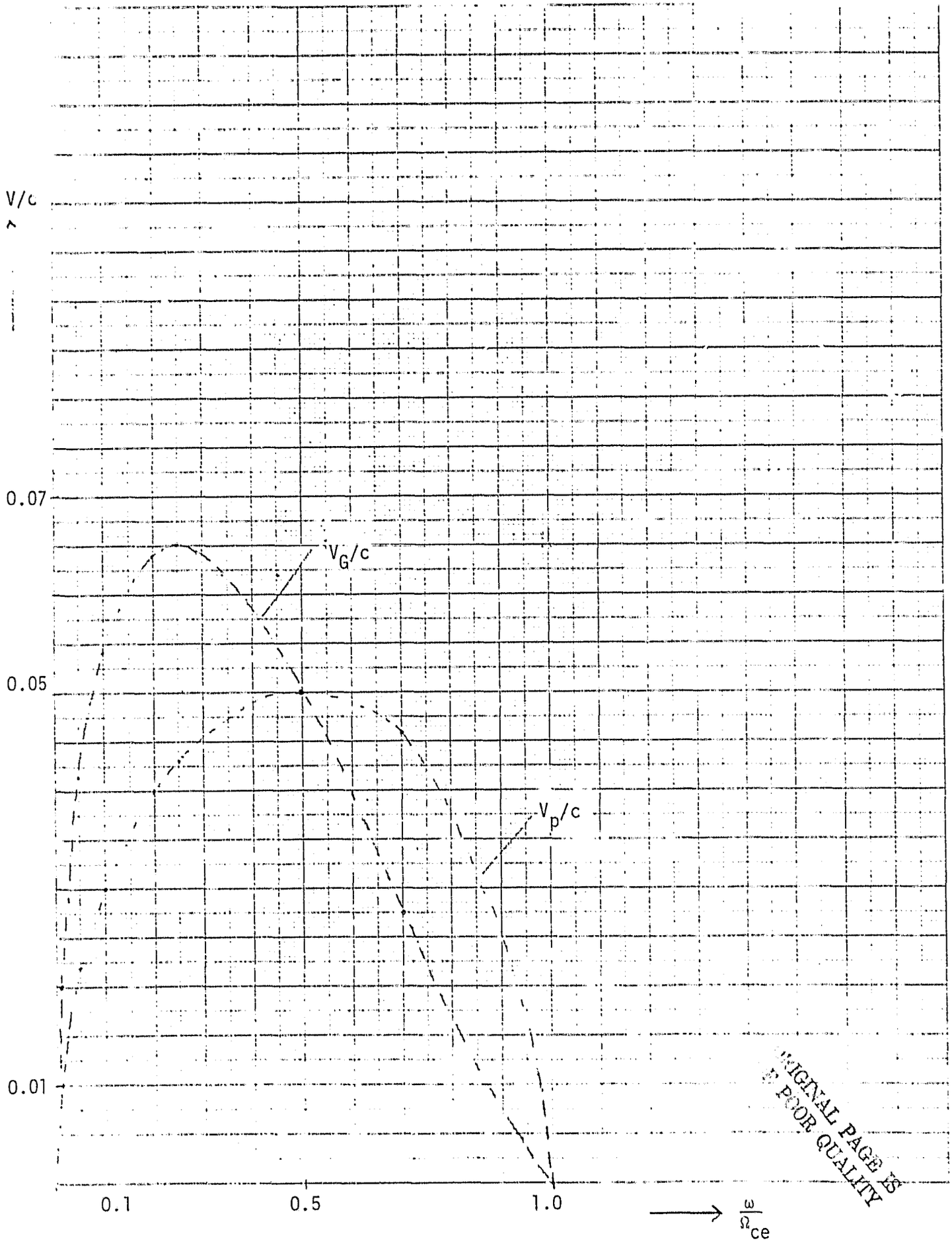

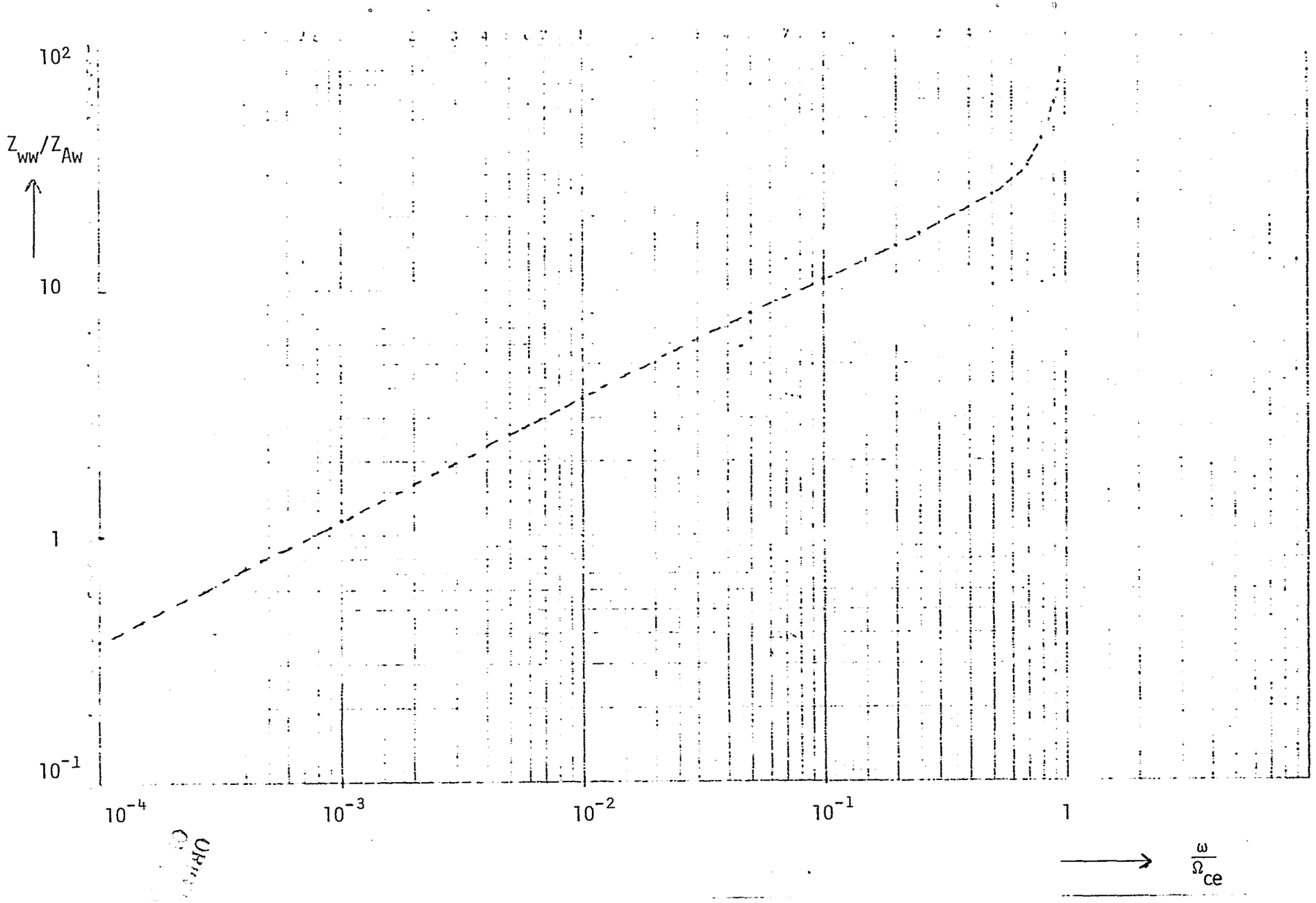

Figure 8. Ratio of whistler (Z_{ww}) to Alfvèn wave (Z_{Aw}) impedance, versus normalized frequency ω/Ω_c.